Bioorganic Chemistry 84 (2019) 309–318

Contents lists available at ScienceDirect

Bioorganic Chemistry

journal homepage: www.elsevier.com/locate/bioorg

New tirucallane triterpenoids from *Picrasma quassioides* with their potential antiproliferative activities on hepatoma cells

Wen-Yu Zhao[a], Jing-Jie Chen[a], Chun-Xin Zou[a], Ying-Ying Zhang[a], Guo-Dong Yao[a], Xiao-Bo Wang[b], Xiao-Xiao Huang[a,b,*], Bin Lin[c,*], Shao-Jiang Song[a,*]

[a] School of Traditional Chinese Materia Medica, Key Laboratory of Computational Chemistry-Based Natural Antitumor Drug Research & Development, Liaoning Province, Shenyang Pharmaceutical University, Shenyang 110016, People's Republic of China
[b] Chinese People's Liberation Army 210 Hospital, Dalian 116021, People's Republic of China
[c] School of Pharmaceutical Engineering, Shenyang Pharmaceutical University, Shenyang 110016, People's Republic of China

ARTICLE INFO

Keywords:
Tirucallane triterpenoids
Picrasma quassioides
Cytotoxicity
Anti-hepatoma

ABSTRACT

Seven new tirucallane-type triterpenoids (**1**–**7**), kumuquassin A-G, along with 20 known analogues (**8**–**27**) were isolated from the stems of *Picrasma quassioides*. The structures and the absolute configurations of new compounds were elucidated by spectroscopic data, electronic circular dichroism (ECD) spectroscopic analyses and quantum ECD calculations. Notably, kumuquassin A (**1**) contains a rare $\Delta^{17,20}$ double bond, kumuquassin B (**2**) is the first example of tirucallane triterpenoid possessing a 5/3 biheterocyclic ring system at the side chain. All the compounds were screened for the cytotoxicity against two human hepatoma cell lines, HepG2 and Hep3B, and several compounds exhibited promising activity. The most potential compound **3** was selected for cell cycle analysis, which showed that **3** could cause an accumulation of HepG2 cells at subG1 peak. Annexin V-FITC/PI staining further confirmed that compound **3** caused death of hepatoma cells through apoptosis induction.

1. Introduction

The plant *Picrasma quassioides* (family Simaroubaceae), a perennial small arbor, is widely distributed throughout temperate and subtropical countries such as China, India, Korean and Japan [1]. As a Traditional Chinese Medicine, the stems of this plant have been used as vermicide, anti-inflammatory and antibacterial agents [2]. Previous investigation showed that alkaloids and quassinoids were the principal active components in *P. quassioides* [2–5]. Recently, several tirucallane triterpenoids have been isolated from plants in the family Simaroubaceae [6,7]. Those compounds play important roles in plant chemotaxonomy and exhibit significant cytotoxicity against various types of cancer cells [8].

In our previous study, several alkaloids with potential anti-hepatoma activity have been obtained from *P. quassioides* [9]. During our continuing search for structurally intriguing and potential anti-hepatoma natural products from Traditional Chinese Medicine plants, we re-examined the chemical constituents of *P. quassioides*. In this study, we describe the isolation and structural elucidation of 7 new tirucallane-type triterpenoids (**1**–**7**), along with 20 known analogues (**8**–**27**) from the stems of *P. quassioides*. Among the isolated compounds, **1** features $\Delta^{17,20}$ double bond, which was the first example in tirucallane triterpenoids from plants; compound **2** was the first derivative of tirucallane triterpenoids with an unprecedented 5/3 biheterocyclic ring system at the side chain. All the isolates were screened *in vitro* for their cytotoxicity against two human hepatoma cell lines, HepG2 and Hep3B. As a preliminary investigation of the mechanism, cell cycle and apoptosis analyses were performed.

2. Experimental section

2.1. General experimental procedures

UV spectra were recorded using an UV-1700 spectrophotometer (SHIMADZU, Japan). IR spectra were obtained on a Bruker IFS 55 spectrophotometer (Bruker, Germany). Optical rotations were measured using an AUTOPOL IV automatic polarimeter (Rudolph Research Analytical, USA). ECD spectrum was recorded on a MOS-450 spectrometer (Bio-Logic Science, France). NMR experiments were performed on Bruker ARX-400 and AV-600 spectrometers. HRESIMS was acquired in the positive-ion mode on a Bruker Micro Q-TOF spectrometer. Column chromatography was performed on silica gel (100–200 or 200–300 mesh; Qingdao Marine Chemical Inc. China). Semi-

* Corresponding authors at: School of Traditional Chinese Materia Medica, Key Laboratory of Computational Chemistry-Based Natural Antitumor Drug Research & Development, Liaoning Province, Shenyang Pharmaceutical University, Shenyang 110016, People's Republic of China (X X. Huang).
E-mail addresses: xiaoxiao270@163.com (X.-X. Huang), randybinlin@163.com (B. Lin), songsj99@163.com (S.-J. Song).

https://doi.org/10.1016/j.bioorg.2018.11.049
Received 6 September 2018; Received in revised form 6 October 2018; Accepted 25 November 2018
Available online 28 November 2018
0045-2068/

preparative HPLC was run on a Shimadzu LC-20A equipped with an SPD-20A UV/VIS detector using an YMC Pack ODS-A column (250 × 10 mm, 5 μm).

2.2. Plant material

The dried stems of *P. quassioides* were collected in November 2015 from Bozhou, Anhui Province, People's Republic of China, and were identified by Prof. Jin-Cai Lu (School of Traditional Chinese Materia Medica, Shenyang Pharmaceutical University). A voucher specimen (20151101) was deposited at the Department of Natural Products Chemistry, Shenyang Pharmaceutical University.

2.3. Extraction and isolation

The air-dried stems from *P. quassioides* (30.0 kg) were extracted three times with 95% aqueous ethanol (50 L). The extract (1200 g) was separated by vacuum liquid chromatography (silica gel 100–200 mesh), eluting with CH_2Cl_2/MeOH (1:0 to 0:1 v/v) and afforded four fractions, A-D. Fraction A (180.0 g) was chromatographed over polyamide column (200–300 mesh) eluted with EtOH-H_2O (3:7 to 9:1) and afforded two fractions, A1 and A2, and fraction A2 (120 g) was further separated on repeated silica gel eluted with PE-acetone to obtain A2-1, A2-2, A2-3. Then Fr. A2-1 (38.0 g) was fractioned by RP-C18 CC (MeOH-H_2O, 20:80–100:0, v/v) into three parts named A2-1a, A2-1b and A2-1c. Sequential separation of A2-1c (26.0 g) over silica gel (PE-EtOAc, 20:1–1:1, v/v) yielded nine fractions (A2-1c-1 to A2-1c-9). Fr A2-1c-5 (0.6 g) was purified through preparative HPLC (MeCN-H_2O, 78:22, v/v) to give compounds **5** (62.4 mg) and **16** (85.0 mg). Similarly, Fr. A2-1c-6 (1.3 g) was purified by HPLC chromatography (MeCN-H_2O, 75:25, v/v) to afford **14** (9.8 mg), **17** (18.5 mg), **18** (8.0 mg) and **24** (6.8 mg). A2-1c-7 (1.6 g) was separated by HPLC eluted with MeCN-H_2O (70:30) to afford **10** (55.0 mg), **15** (13.1 mg), **19** (12.0 mg), **25** (59.6 mg) and **26** (25.0 mg). A2-1c-8 (1.4 g) was purified by semi-preparative HPLC (MeCN-H_2O, 75:25) to give **9** (28.7 mg), **11** (55.3 mg), **20** (12.3 mg), **21** (147.6 mg) and **27** (46.1 mg). Compound **22** (40.7 mg) was obtained from Fr. A2-1c-9 (200.4 mg) via preparative HPLC (MeCN-H_2O, 72:28, v/v).

Fraction A2-2 (23.0 g) was chromatographed on RP-C_{18} silica gel eluted with a gradient of MeOH/H_2O (20:80 to 100:0) to yield three fractions, A2-2a to A2-2c. Subfraction A2-2c (12.3 g) was separated by a silica gel column eluted with gradient mixtures using increasing amounts of EtOAc (0–100%) in PE to afford fifteen fractions, A2-2c-1 to A2-2c-15. Compounds **8** (3.2 mg) and **13** (10.3 mg) were obtained from Fr. A2-2c-4 (407.9 mg) via preparative HPLC (MeCN-H_2O, 70:30, v/v). Fr A2-2c-7 (620.2 mg) was purified through preparative HPLC (MeCN-H_2O, 68:32, v/v) to give compounds **3** (3.2 mg) and **4** (4.4 mg). Fraction A2-2c-11 (1.2 g) was separated by preparative HPLC (MeOH-H_2O, 82:18) to give **2** (4.9 mg) and **12** (22.3 mg). Compounds **1** (10.1 mg) and **6** (10.6 mg) were purified from Fr. A2-2c-12 (480.6 mg) via preparative HPLC (MeCN-H_2O, 65:35, v/v). A2-2c-15 (182.3 mg) was separated by HPLC (MeOH-H_2O, 80:20) yield **7** (8.7 mg).

Kumuquassin A ***(1)*** Light yellow powder. $[\alpha]_D^{20}$ −42.3 (*c* 0.10, MeOH); UV (MeOH) λ_{max} (log ε) 236 (1.14) nm; IR (KBr) ν_{max} 3430, 2987, 2830, 1608, 1492, 1441, 1400, 1367, 1173, 1007 cm^{-1}; ^1H and ^{13}C NMR data, see Tables 1 and 2; HRESIMS *m/z* 507.3079 $[M + Na]^+$ (calcd for $C_{30}H_{44}O_5Na$, 507.3081).

Kumuquassin B ***(2)*** White powder. $[\alpha]_D^{20}$ −12.4 (*c* 0.10, MeOH); UV (MeOH) λ_{max} (log ε) 201 (3.92) nm; IR (KBr) ν_{max} 3435, 2986, 1608, 1492, 1441, 1400, 1385, 1367, 1173, 1006, 799 cm^{-1}; ^1H and ^{13}C NMR data, see Tables 1 and 2; HRESIMS *m/z* 525.3188 $[M + Na]^+$ (calcd for $C_{30}H_{46}O_6Na$, 525.3187).

Kumuquassin C ***(3)*** White powder. $[\alpha]_D^{20}$ −18.9 (*c* 0.10, MeOH); UV (MeOH) λ_{max} (log ε) 230 (1.13) nm; ^1H and ^{13}C NMR data, see Tables 1 and 2; HRESIMS *m/z* 485.3225 $[M + Na]^+$ (calcd for $C_{30}H_{45}O_5Na$, 485.3262).

Kumuquassin D ***(4)*** White powder. $[\alpha]_D^{20}$ −22.7 (*c* 0.10, MeOH); UV (MeOH) λ_{max} (log ε) 201 (4.02) nm; IR (KBr) ν_{max} 3446, 2986, 2831, 1607, 1492, 1441, 1399, 1385, 1367, 1173, 1006, 799 cm^{-1}; ^1H and ^{13}C NMR data, see Tables 1 and 2; HRESIMS *m/z* 509.3225 $[M + Na]^+$ (calcd for $C_{30}H_{46}O_5Na$, 509.3237).

Kumuquassin E ***(5)*** Yellow powder. $[\alpha]_D^{20}$ −15.4 (*c* 0.10, MeOH); UV (MeOH) λ_{max} (log ε) 201 (4.19) nm; IR (KBr) ν_{max} 3437, 2968, 2926, 1633, 1460, 1376, 1236, 1159 cm^{-1}; ^1H and ^{13}C NMR data, see Tables 1 and 2; HRESIMS *m/z* 463.3549 $[M + Na]^+$ (calcd for $C_{30}H_{48}O_2Na$, 463.3547).

Kumuquassin F ***(6)*** Yellow powder. $[\alpha]_D^{20}$ −38.6 (*c* 0.10, MeOH); UV (MeOH) λ_{max} (log ε) 201 (4.37) nm; IR (KBr) ν_{max} 3433, 2985, 2950, 1607, 1492, 1441, 1400, 1385, 1367, 1173, 1006, 799 cm^{-1}; ^1H and ^{13}C NMR data, see Tables 1 and 2; HRESIMS *m/z* 479.3499 $[M + Na]^+$ (calcd for $C_{30}H_{48}O_3Na$, 479.3496).

Kumuquassin G ***(7)*** White powder. $[\alpha]_D^{20}$ −13.4 (*c* 0.10, MeOH); UV (MeOH) λ_{max} (log ε) 201 (4.17) nm; IR (KBr) ν_{max} 3431, 2985, 2948, 1607, 1492, 1441, 1401, 1367, 1173, 1007, 798 cm^{-1}; ^1H and ^{13}C NMR data, see Tables 1 and 2; HRESIMS *m/z* 481.3645 $[M + Na]^+$ (calcd for $C_{30}H_{50}O_3Na$, 481.3652).

2.4. ECD calculations

Conformational searches were run with CONFLEX using the Merck molecular force field (MMFF) with standard parameters [10]. Conformers with a Boltzmann distribution ≥1% were chosen. The conformers were then imported into Gaussian 09 software and optimized at the B3LYP/6-31G(d) levels [11]. The ECD curves of the conformers were determined by the TDDFT method at the B3LYP/6-311 + + G (2d, p) level with the CPCM model in a methanol solution.

2.5. Cell culture

HepG2 and Hep3B cells were obtained from Chinese Academy of Sciences (Shanghai, China). The cells were cultured in DMEM medium supplemented with 10% FBS, 10 mg/mL streptomycin, 100 U/ml penicillin and maintained at 37 °C with 5% CO_2 at a humidified atmosphere. Logarithmically growing cells were used in all the experiments.

2.6. SRB assay

The HepG2 and Hep3B cells were treated with compounds and sorafenib for 48 h. Then 50% Trichloroacetic acid was added to the culture medium, for 1 h at 4 °C. The plates were then washed with tap water to remove TCA, air-dried and stained for 30 min with 0.4% SRB dissolved in 1% acetic acid. After incubation, the cultures were rinsed with 1% acetic acid to remove residual dye. The plates were air-dried and the bound dye was solubilized with 200 μL of 10 mM Tris base solution (pH 10.5). The absorbance of each well was determined at 540 nm using a microplate reader (Thermo Scientific Multiskan MK3, Shanghai, China).

2.7. Cell cycle analysis

HepG2 cells were seeded in 6-well plates (2.5×10^5 cells/well), incubated in the presence or absence of compound **3** at the indicated concentrations for 24 h, harvested by centrifugation, and then fixed in ice-cold 70% ethanol overnight. After the ethanol was removed the next day, the cells were resuspended in ice-cold PBS, treated with RNase A (Keygen Biotech, China) at 37 °C for 30 min, and then incubated with the DNA staining solution propidium iodide (PI, Keygen Biotech, China) at 4 °C for 30 min. Approximately 10,000 events were detected by flow cytometry (Beckman Coulter, Epics XL).

Table 1
^{1}H NMR (600 MHz) data of compounds **1–7** in $CDCl_3$ (δ in ppm, J in Hz).

No.	1	2	3	4	5	6	7
1α	1.48, td (13.5, 3.6)	1.46, m	1.42, m	1.46, m	1.44, m	1.46, m	1.13, m
β	1.99, ddd (13.5, 5.4, 3.6)	1.98, m	1.98, m	1.98, m	1.96, m	1.99, m	1.67, m
2α	2.26, dt (14.5, 3.6)	2.24, dt (14.0, 3.1)	2.24, dt (14.3, 3.6)	2.25, m	2.21, dt (14.3, 3.6)	2.24, m	1.31, m
β	2.76, td (14.5, 5.4)	2.75, td (14.0, 5.5)	2.75, td (14.3, 5.5)	2.76, td (14.5, 5.5)	2.72, td (14.3, 5.5)	2.74, dd (14.4, 5.4)	1.64, m
3							3.24, dd (11.5, 4.1)
5	1.75, m	1.72, t (8.8)	1.71, m	1.75, m	1.69, m	1.72, m	1.31, m
6α	2.11, m	2.10, m	2.10, m	2.10, m	2.08, m	2.09, m	1.94, m
β	2.11, m	2.10, m	2.11, m	2.11, m	2.08, m	2.10, m	2.10, m
7	5.43, q (3.4)	5.30, br d (3.3)	5.33, br d (3.3)	5.33, br d (3.2)	5.28, q (3.3)	5.31, overlap	5.27, q (3.2)
9	2.35, m	2.32, m	2.25, m	2.31, m	2.25, m	2.26, m	2.18, m
11α	1.70, m	1.59, m	1.57, m	1.60, m	1.52, m	1.57, m	1.52, m
β	1.74, m	1.59, m	1.57, m	1.60, m	1.52, m	1.57, m	1.52, m
12α	1.74, m	2.10, m	2.07, m	1.82, m	1.80, m	1.83, m	1.79, m
β	1.74, m	1.59, m	1.39, m	1.82, m	1.62, m	1.83, m	1.62, m
15α	2.92, m	1.54, m	1.61, m	1.59, m	1.48, m	1.50, m	1.50, m
β	3.05, m	1.60, m	1.67, m	1.65, m	1.48, m	1.50, m	1.50, m
16α	1.71, m	1.40, m	1.79, m	1.83, m	1.22, m	1.70, m	2.04, m
β	2.11, m	1.64, m	2.03, m	1.88, m	2.01, m	1.83, m	2.11, m
17		2.82, t (9.2)	2.96, t (9.3)	2.01, m	1.44, m	1.78, m	1.77, m
18	1.06, s	0.94, s	0.73, s	0.98, s	0.78, s	0.81, s	0.83, s
19	1.03, s	1.00, s	1.02, s	1.04, s	0.97, s	0.99, s	0.74, s
20					1.40, m	1.50, m	1.49, m
21		5.34, d (6.1)		5.30, br s	0.82, d (5.9)	3.73, dd (11.1, 3.4), 3.56, dd (11.1, 5.4)	3.75, dd (11.1, 3.2), 3.59, dd (11.1, 5.5)
22α	2.92, m	3.28, s	7.34, br s	2.08, m	1.40, m	1.41, m	1.41, m
β	3.10, m			1.84, m	1.64, m	1.51, m	1.49, m
23	4.74, ddd (8.4, 5.7, 2.0)	4.50, s	3.66, d (4.8)	4.13, m	5.56, m	1.94, m, 1.32, m	1.94, m, 1.31, m
24	3.25, d (2.0)	3.37, br d (6.7)	5.05, m	2.70, d (7.5)	5.55, m	5.33, overlap	5.34, t (7.9)
26	1.37, s	1.32, s	1.37, s	1.33, s	1.28, s	4.13, d (11.8), 4.08, d (11.8)	4.15, d (11.8), 4.11, d (11.8)
27	1.28, s	1.27, s	1.34, s	1.31, s	1.27, s	0.80, s	1.80, s
28	1.06, s	1.04, s	1.05, s	1.05, s	1.01, s	1.03, s	0.98, s
29	1.12, s	1.11, s	1.12, s	1.12, s	1.08, s	1.10, s	0.86, s
30	0.94, s	1.05, s	1.12, s	1.05, s	0.97, s	1.03, s	0.97, s

2.8. Apoptosis analysis

The apoptotic analysis was carried out using an Annexin V-FITC Apoptosis Detection Kit (Bimake, Houston, USA). HepG2 cells were treated with compounds for 48 h. Then the cells were collected, washed with ice-cold PBS and resuspended in AnnexinV-FITC/PI staining solution according to the manufacturer's instructions for 15 min in the dark. The cells were then immediately analyzed with a BD FACS CantoTM flow cytometer (BD Biosciences, New Jersey, USA).

2.9. Statistical analysis

All the presented data and results were confirmed in at least three independent experiments. The data were expressed as means ± SD. Statistical comparisons were analyzed by one-way ANOVA using GraphPad Prism from GraphPad Software (GraphPad software, California, USA). LSD-post hoc test was employed to assess the statistical significance of difference between control and treated groups. $P < 0.05$ was considered statistically significant.

3. Results and discussion

3.1. Structure elucidation

Compound **1** (Fig. 1) had the molecular formula $C_{30}H_{44}O_5$ deduced from its sodium adduct ion peak $[M + Na]^+$ at m/z 507.3079 (calcd for $C_{30}H_{44}O_5Na$, 507.3081) in the HRESIMS experiment, which indicated nine degrees of unsaturation. The ^{1}H NMR spectrum (Table 1) exhibited signals for seven tertiary methyl groups [δ_H 0.94, 1.03, 1.06, 1.06, 1.12, 1.32, and 1.37 (3H, s, for each)], two oxymethine protons [δ_H 3.26 (1H, d, J = 2.0 Hz, H-24) and 4.74 (1H, ddd, J = 8.4, 5.7, 2.0 Hz, H-23)], and a typical signal (δ_H 5.43, m) of an olefinic proton (H-7). All carbons in the molecular structure were resolved as individual resonances in the ^{13}C NMR spectrum (Table 2) and classified using HSQC spectroscopy as seven methyls, seven sp^3 methylenes, four sp^3 methines (two oxygenated at δ_C 76.2 and 77.4), five sp^3 quaternary carbons (including one oxygenated at δ_C 72.7), a sp^2 methylene (δ_C 119.5), three sp^2 quaternary carbon (δ_C 114.0, 143.1, 168.3). The above data indicated that compound **1** possessed the similar scaffold as (23*R*, 24*S*)-21-oxomelianodiol [12], which was a 21, 23-epoxy-tirucalla triterpenoids. The main difference between these two compounds being the presence of a $\Delta^{17,20}$ double bond in **1**. This finding was confirmed by the HMBC correlations (Fig. 2) from δ_H 3.10, 2.92 (H-22) and δ_H 2.11, 1.71 (H-16) to δ_C 168.3, 114.0 (C-17 and C-20, respectively).

The geometry of the double bond $\Delta^{17,20}$ in **1** was assigned as *Z* configuration using the NOESY correlations between H-16 and H-22 (Fig. 3). The relative configuration of **1** was determined on the basis of the NOESY spectrum in combination with couplings in the ^{1}H NMR spectrum. The correlations of H_3-28/H-5 and H-5/H-9 indicated an α-orientation. Cross-peaks between H_3-29/H_3-19, H_3-18/H-15α and H_3-30/H-15β revealed that Me-19 and Me-30 were β-oriented. Additionally, the correlations of H_3-30/H-16β, H-16β/H-22β, H-22β/H-23 and H-23/H-24 suggested β-orientation of H-23 and H-24, which was supported by a clear coupling constant, $J_{H\text{-}23/H\text{-}24}$ of 2.0 Hz in the ^{1}H NMR spectrum.

The absolute configuration of **1** was determined by the comparison of its ECD spectrum with the data calculated using the time-dependent density functional theory (Fig. 4). Thus, **1** was structurally established

Table 2
^{13}C NMR (100 MHz) data of compounds **1–7** in $CDCl_3$ (δ in ppm).

No.	1	2	3[a]	4	5	6	7
1	38.5	38.6	38.7	38.6	38.6	38.6	37.3
2	35.0	35.0	35.0	35.0	35.0	35.0	27.8
3	216.6	216.9	217.0	216.8	217.0	217.1	79.4
4	48.0	48.0	48.0	48.0	47.9	48.0	39.1
5	52.5	52.5	52.6	52.6	52.4	52.4	50.8
6	24.5	24.5	24.5	24.6	24.4	24.4	24.1
7	119.5	118.5	118.5	118.6	117.9	118.2	118.3
8	143.1	145.1	145.5	145.2	146.0	145.8	145.7
9	48.1	48.3	48.5	48.3	48.5	48.5	49.0
10	35.3	35.3	35.3	35.3	35.1	35.1	35.1
11	17.7	17.8	17.6	17.9	18.3	18.3	18.2
12	33.4	31.8	30.6	32.4	34.1	32.9	33.0
13	49.8	45.0	45.2	44.9	43.6	43.4	43.5
14	50.3	51.2	51.2	51.3	51.3	51.4	51.4
15	30.4	34.0	34.4	33.7	33.6	34.0	34.0
16	28.9	21.6	26.6	23.2	28.2	24.5	24.5
17	168.3	41.9	43.8	53.1	52.7	47.3	47.3
18	25.0	24.0	23.3	23.5	22.1	22.3	22.3
19	12.8	12.9	12.9	12.9	12.9	12.9	13.3
20	114.0	67.2	135.9	82.6	36.5	42.5	42.6
21	171.2	96.5	174.0	100.6	18.5	62.7	62.9
22	28.6	58.2	147.5	41.5	38.9	30.1	30.2
23	76.2	78.9	77.0	77.0	125.5	27.9	28.0
24	77.4	74.2	81.0	65.7	139.5	129.1	129.2
25	72.7	74.4	71.8	57.6	70.8	134.4	134.5
26	26.8	26.7	28.4	25.1	30.0	61.7	61.9
27	27.0	26.5	24.8	19.5	30.1	21.8	21.7
28	24.7	24.7	24.7	24.7	24.6	24.7	27.7
29	21.7	21.7	21.7	21.7	21.7	21.7	14.9
30	27.2	27.6	27.7	27.7	27.5	27.6	27.5

[a] Measured at 150 MHz.

as (17*Z*, 23*S*, 24*S*)-24, 25-dihydroxy-3-oxo-tirucalla-7, 17-dien-21, 23-olide and was conferred the trivial name Kumuquassin A. Kumuquassin A (**1**) contains a rare $\Delta^{17,20}$ double bond, which was the first example in tirucallane triterpenoids from plants.

Compound **2** was assigned the molecular formula $C_{30}H_{46}O_6$ on the basis of HRESIMS $[M + Na]^+$ signal at *m/z* 525.3188 (calcd for $C_{30}H_{46}O_6Na$, 525.3187), which indicated eight indices of hydrogen deficiency. Analysis of its NMR spectroscopic data (Tables 1 and 2) suggested that **2** was a tirucallane-type triterpenoid with a typical $\Delta^{7,8}$ double bond. Comparison of the spectroscopic data of **2** and meliandiol (**12**) [13] revealed that they possessed the same 21, 23-epoxy moiety and carbonyl at C-3. Five rings and two double bonds accounted for seven of the eight degrees of unsaturation, with the last degree of unsaturation requiring an additional ring. An oxygenated quaternary carbon (δ_C 67.2) and an oxygenated methine (δ_C 58.2) were observed in ^{13}C NMR and HSQC spectrum, which suggested a three-membered *O*-heterocyclic ring at C-20. These observations were supported by the HMBC data (Fig. 2). The correlations from the proton signals at δ_H 5.34 (H-21) and 4.50 (H-23) to the carbon signal at δ_C 67.2 (C-20), and the cross-peak of the oxygenated methine proton signal at δ_H 3.28 (H-22) with the signal at δ_C 78.9 (C-23) substantiated the presence of 20, 21-epoxy moiety.

ROESY experiments were conducted to determine the configurations at the stereocenters in **2** (Fig. 3). The correlations of Me-30/H-17, H-17/H-22, H-22/H-23 and H-23/H-24 indicated the β-orientation of H-22, H-23 and H-24, which was further supported by the singlet peaks of H-22 (δ_H 3.28) and H-23 (δ_H 4.50) in ^{1}H NMR. Thus, the structure of Kumuquassin B (**2**) was established as (20*S*, 21*S*, 22*S*, 23*R*, 24*S*)-21, 24, 25-trihydroxy-20, 22: 21, 23-diepoxytirucall-7-en-3-one. Compound **2** was the first natural occurring derivative of tirucallane triterpenoid possessing a novel 5/3 biheterocyclic ring system at the side chain.

Kumuquassin C (**3**) was assigned a molecular formula of $C_{30}H_{44}O_5$, on the basis of the HRESIMS at *m/z* 485.3225 $[M + H]^+$ (calcd for $C_{30}H_{45}O_5$, 485.3262). The spectroscopic data (Tables 1 and 2) of **3** were similar to those of dysolenticin B [14], except for the $\Delta^{24,25}$ double bond in dysolenticin B was replaced by 1, 2-diol group in compound **3**. The structure was supported by HMBC correlations (Fig. 2) between δ_H 3.65 (H-23) and δ_C 81.0 (C-24) and 71.8 (C-25). In the ^{1}H NMR spectrum, a clear coupling constant, $J_{H\text{-}23/H\text{-}24}$, of 4.8 Hz indicated the *trans-gauche* configuration of the side-chain in **3**. However, the configurations of C-23 and C-24 were difficult to establish directly from the NOESY spectrum since the distance between C-17 and C-23 is too far. In light of this, we performed quantum-mechanical ECD calculations with the time-dependent DFT method to establish the absolute configuration of **3**. The respective calculated ECD spectra of the two possible diastereoisomers of **3** (**3a** and **3b**, Fig. 5**A**) were brought into comparisons with the experimental data. As shown in Fig. 5**B**, the ECD profile of **3a** (23*S*, 24*R*) was in agreement with the experimental data. Then, the structure as well as the configurations of picraquassin O (**3**) were undoubtedly established as (23*S*, 24*R*)-24, 25-dihydroxy-3-oxo-tirucalla-7, 20 (22)-dien-21, 23-olide.

Compound **4** was conferred a molecular formula of $C_{30}H_{46}O_5$ on the basis of the HRESIMS at *m/z* 509.3225 $[M + Na]^+$ (calcd for $C_{30}H_{46}O_5$, 509.3237). Comparison of its 1D NMR (Tables 1 and 2) and HSQC data with those of melianone (**9**) [15] revealed that protons at C-20 in the latter compound is substituted with an additional hydroxyl group in **4**. The HMBC correlations (Fig. 2) from δ_H 2.01 (H-17) and 5.30 (H-21) to the oxygenated carbon signal at δ_C 82.6 (C-20) verified the location of a hydroxy at C-20. The NOESY correlations (Fig. 6) of Me-30/H-17, H-17/H-21, H-17/H-22β, H-22β/H-24 and H-24/Me-26 suggested the protons of H-21 and H-24 are β-oriented in **4**. Moreover, the configuration of H-24 was confirmed on the basis of the coupling constant ($J_{H\text{-}23/H\text{-}24}$ = 7.6 Hz) in the ^{1}H NMR spectrum. Accordingly, compound **4** (Kumuquassin D) was structurally determined as (20*R*, 21*R*, 23*R*, 24*S*)-20, 21-dihydroxy-21, 23: 24, 25-diepoxytirucall-7-en-3-one.

Compound **5** was isolated as a white powder, and its molecular formula was determined as $C_{30}H_{48}O_2$ on the basis of a HRESIMS peak at *m/z* 463.3549 $[M + Na]^+$ (calcd for $C_{30}H_{48}O_2Na$, 463.3547). The ^{1}H and ^{13}C NMR spectra of **5** (Tables 1 and 2) were similar to those of (23*E*)-3β, 25-dihydroxytirucalla-7, 23-diene [6] except for the addition of a ketone group at C-3 (δ_C 217.0). The stereochemistry of **5** was consistent with that of (23*E*)-3β, 25-dihydroxytirucalla-7, 23-diene, as established based on their comparable 1D-NMR and NOESY spectra (Fig. 6) [16]. Consequently, the structure of compound **5** (Kumuquassin E) was proposed as (23*E*)-25-hydroxytirucalla-7, 23-dien-3-one.

Kumuquassin F (**6**) was found to possess a molecular formula of $C_{30}H_{48}O_3$ by HRESIMS at *m/z* 479.3499 $[M + Na]^+$ (calcd for $C_{30}H_{48}O_3Na$, 479.3496). The 1D- and 2D-NMR spectra of compound **6** closely resembled those of (24*Z*)-27-hydroxy-7, 24-tirucalladien-3-one [17]. The difference was the downfield-shifted resonance of C-21 in **6**, which suggested the replacement of the methyl group at C-21 in (24*Z*)-27-hydroxy-7, 24-tirucalladien-3-one with a hydroxymethyl group in **6**. This deduction was confirmed by the key HMBC correlations (Fig. 2) from the methylene proton signals at δ_H 3.56 (H-21a) and 3.73 (H-21b) to the carbon signal at δ_C 47.3 (C-17) and 42.5 (C-20). The geometry of the double bond $\Delta^{24,25}$ was assigned as *Z* configuration using the NOESY correlations (Fig. 6) between H-24 and Me-27. The absolute configuration at C-20 in tirucallane-type triterpenoids is *S*. Therefore, the structure of compound **6** was established to be (20*S*, 24*Z*)-21, 26-dihydroxytirucalla-7, 24-dien-3-one.

Compound **7** was obtained as a white powder. A sodium adduct ion peak $[M + Na]^+$ at *m/z* 481.3645 (calcd for $C_{30}H_{50}O_3Na$, 481.3652) in the HRESIMS was used to assign a molecular formula of $C_{30}H_{50}O_3$. The NMR spectra (Tables 1 and 2) of **7** were analogous to those of **6** with the primary difference being the absence of signals for a carbonyl group and the presence of a hydroxy at C-3. This conclusion was confirmed by the related HMBC correlations (Fig. 2) from the proton signal at δ_H 0.98 (Me-28) and δ_H 1.67, 1.13 (H-1) to the carbon signal at δ_C 79.4 (C-3). The configuration of hydroxy at C-3 was determined as β-orientation basing on the cross-peak of H-3/H-5 in NOESY spectrum (Fig. 6). The

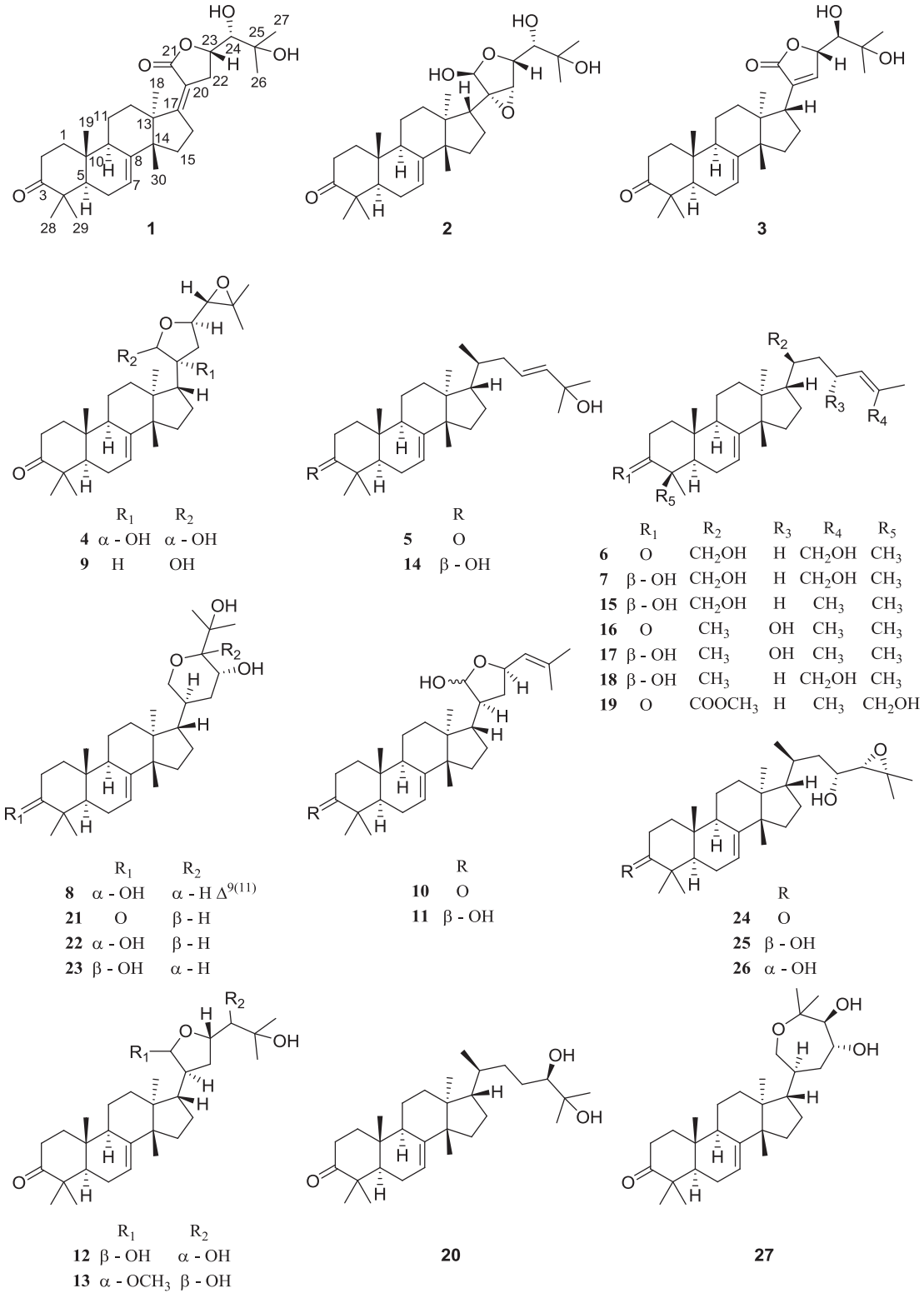

Fig. 1. The structures of compounds **1–27**.

configuration of side-chain was confirmed to be the same as that of **6** based on the results of NOESY experiments and similar 1D-NMR. Thus, compound **7** was established as (20*S*, 24*Z*)-3*β*, 21, 26-trihydroxytirucalla-7, 24-diene and named as Kumuquassin G.

Compound **8** was first obtained from the oxidation of sapelin A (**22**) [18]. It was isolated from natural sources, which has been fully spectroscopically characterized for the first time (Table S1, Supporting Information).

Structure elucidation of the known compounds (**9–27**) was carried out by a combination of spectroscopic means (HRESIMS, ^{1}H and ^{13}C NMR) and comparison with references. The compounds were determined to be melianone (**9**) [15], flindissone (**10**) [19], 3-*epi*-flindissol (**11**) [20], melianodiol (**12**) [13], 21*α*-methylmelianodiol (**13**) [21], 3*β*, 25-dihydroxy-tirucalla-7, 23-diene (**14**) [22], 3*β*-hydroxyl-

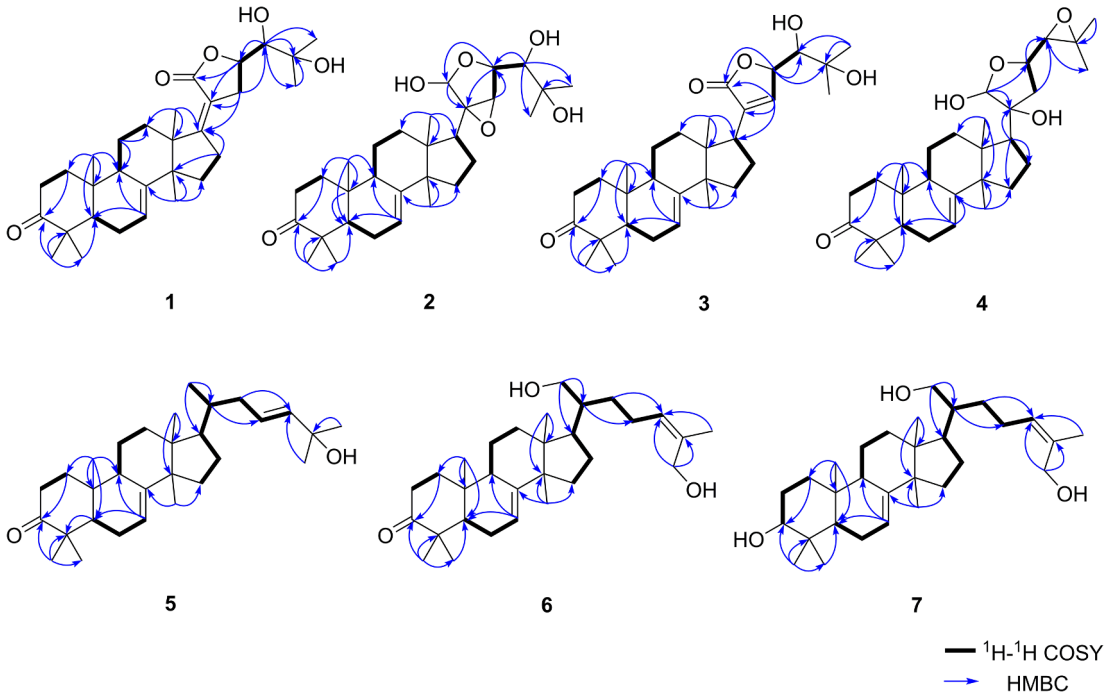

Fig. 2. Key ^{1}H–^{1}H COSY and HMBC correlations of compounds **1**–**7**.

tirucalla-7, 24-dien-21-ol (**15**) [23], 3-oxotirucalla-7, 24-dien-23-ol (**16**) [19], 3*β*, 23-dihydroxy-tirucalla-7, 24-diene (**17**) [22], (24*Z*)-7, 24-tirucalladiene-3*β*, 27-diol (**18**) [17], 29-hydroxy-3-oxotirucalla-7, 24-diene 21-methyl ester (**19**) [7], altissimanins B (**20**) [24], bourjotinolone A (**21**) [25], sapelins A (**22**) [25], 3-episapelins A (**23**) [26], niloticin (**24**) [27], dihydroniloticin (**25**) [26], dyvariabilins G (**26**) [28], and hispidone (**27**) [26].

3.2. Cytotoxicity assay

The crude extract of *P. quassioides* have shown potential anti-hepatoma effect *in vitro* in our previous study [9]. In addition, the tirucallane triterpenoids isolated from the Simarubaceae family have been reported to show strong cytotoxic activities in various types of cancer cell lines [7,26,29], which inspired our study on cytotoxic activity of these compounds. Inhibitory activity of compounds **1**–**27** was evaluated against the HepG2 and Hep3B cells. As shown in Fig. 7, compounds **3**, **6**, **12**, **13** and **21** showed cytotoxic activities towards HepG2 cells with IC_{50} values ranging from 21.72 to 44.19 μM, while **2**, **3**, **6**, **12**, **19** and **24** showed moderate activities against Hep3B with IC_{50} values less than 50 μM. Compound **3** with the most pronounced activity against HepG2 cells (IC_{50}, 21.72 μM) possess an *α*,*β*-unsaturated γ-lactone in side chain, which suggests that this functionality, usually a Michael acceptor, may play a significant role in mediating the activity. However, an *α*,*β*-unsaturated lactone at C-17, C-20 and C-21 was not helpful to the cytotoxic activity since compound **1** did not exhibit antiproliferative effect at 50 μM. It should be noted that compound **21** with a carbonyl group at C-3 showed stronger inhibitory activity than its saturated analogue **22**. A similar behavior was observed for compound **6** compared with **7** (> 50 μM).

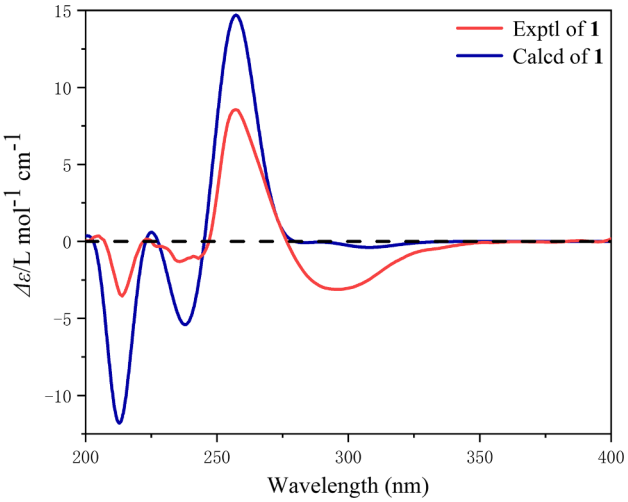

Fig. 4. Experimental and calculated ECD spectra of compound **1** in MeOH.

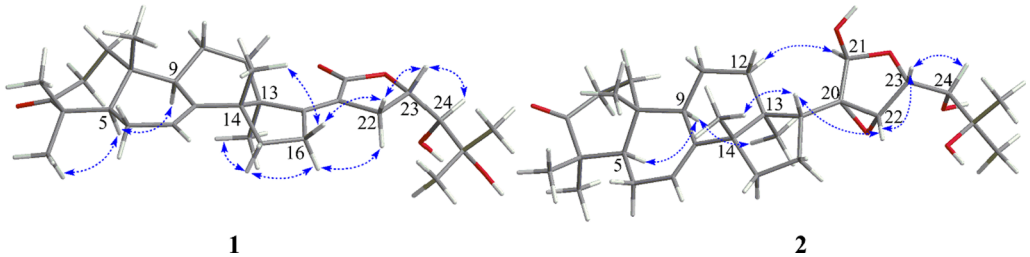

Fig. 3. Key NOESY correlations of **1** and key ROESY correlations of **2**.

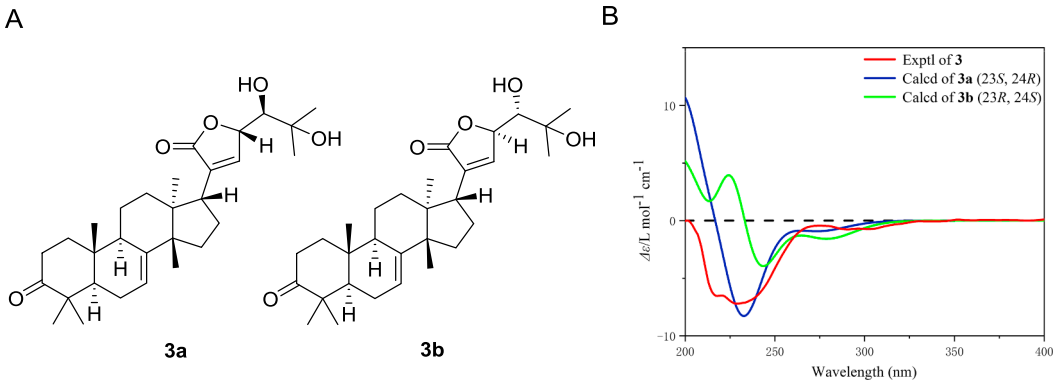

Fig. 5. Determination of the absolute configuration of **3**. A: The structures of **3a** and **3b**. B: Comparison of the calculated ECD spectra of **3a** and **3b** with the experimental spectrum of **3** obtained in MeOH.

3.3. Cell cycle analysis

Cellular proliferation involving the cell division and replication are generally linked to cell cycle progression [30]. To clarify the cytotoxic mechanism of compound **3**, the cell cycle progression of HepG2 cells was analyzed by flow cytometry. The cells were incubated for 48 h with concentrations close to the IC_{50} values or higher of compound **3** (20 and 40 μM). As shown in Fig. 8, a sub-G1 peak was observed at a high concentration (40 μM), as well as a significant decrease in G1 phase. Thus, it is deduced that **3** probably inhibited the proliferation of HepG2 cells via apoptosis induction.

3.4. Apoptosis analysis

Based on the results of cell cycle analysis, an Annexin V-FITC/PI double staining assay was proceeded to evaluate the pro-apoptotic effect of compound **3**. Treatment with **3** (20 and 40 μM) for 48 h induced an accumulation of apoptotic cells compared with the control (Fig. 9**A**). The percentages of apoptotic cells were 31.9% for **3** at 40 μM (Fig. 9**B**), compared with 9.66% in the untreated control cells. These results therefore demonstrated that compound **3** mediated its activity toward HepG2 cells through cell apoptosis induction.

4. Conclusion

In the current study, a total of 27 tirucallane-type triterpenoids (**1**–**27**) were isolated from the stems of *P. quassioides*. Seven of which are new compounds. All isolates were screened for antiproliferative activities against HepG2 and Hep3B cells, and new compound **3** showed significant and selective inhibitory activity towards HepG2 cells. Further mechanistic studies revealed that treatment with **3** induced apoptosis of hepatoma cells. Based on the above evidence, the molecule might represent a valuable complement to current chemotherapies.

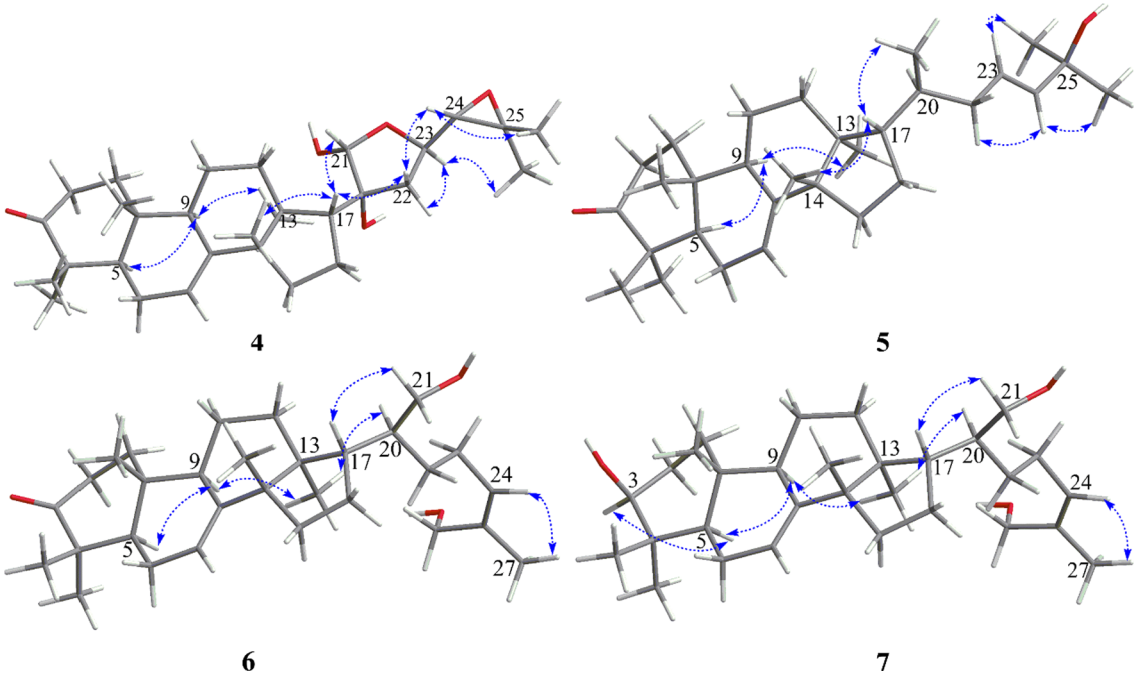

Fig. 6. Key NOESY correlations of compounds **4**–**7**.

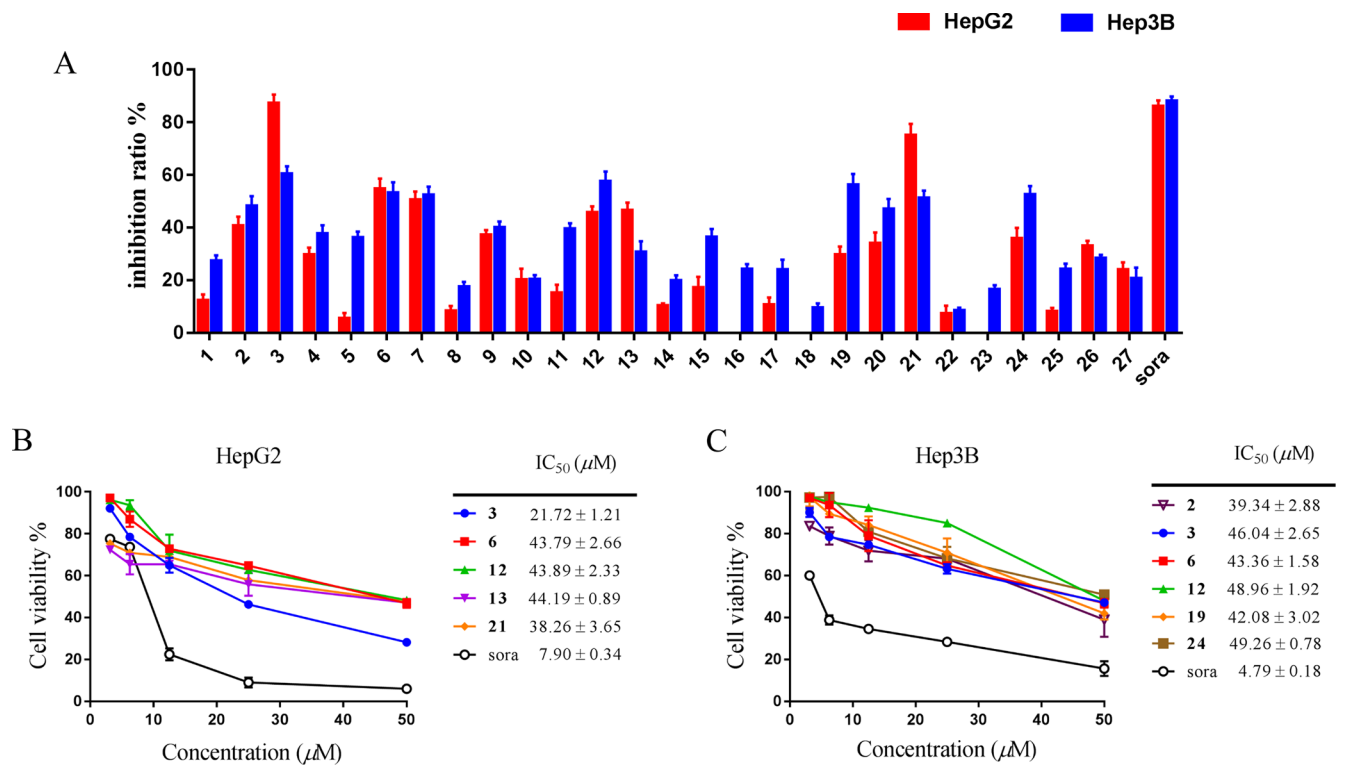

Fig. 7. Cytotoxic activities of compounds **1–27** against two hepatocellular carcinoma cell lines. (A) Inhibition ratio of all isolates at 50 μM. Sora: sorafenib at 12.5 μM, positive control. (B-C) The compounds with inhibition ratio > 40% were screened out to treat HepG2 and Hep3B cells in subsequent experiment and cell viability was determined by SRB assays.

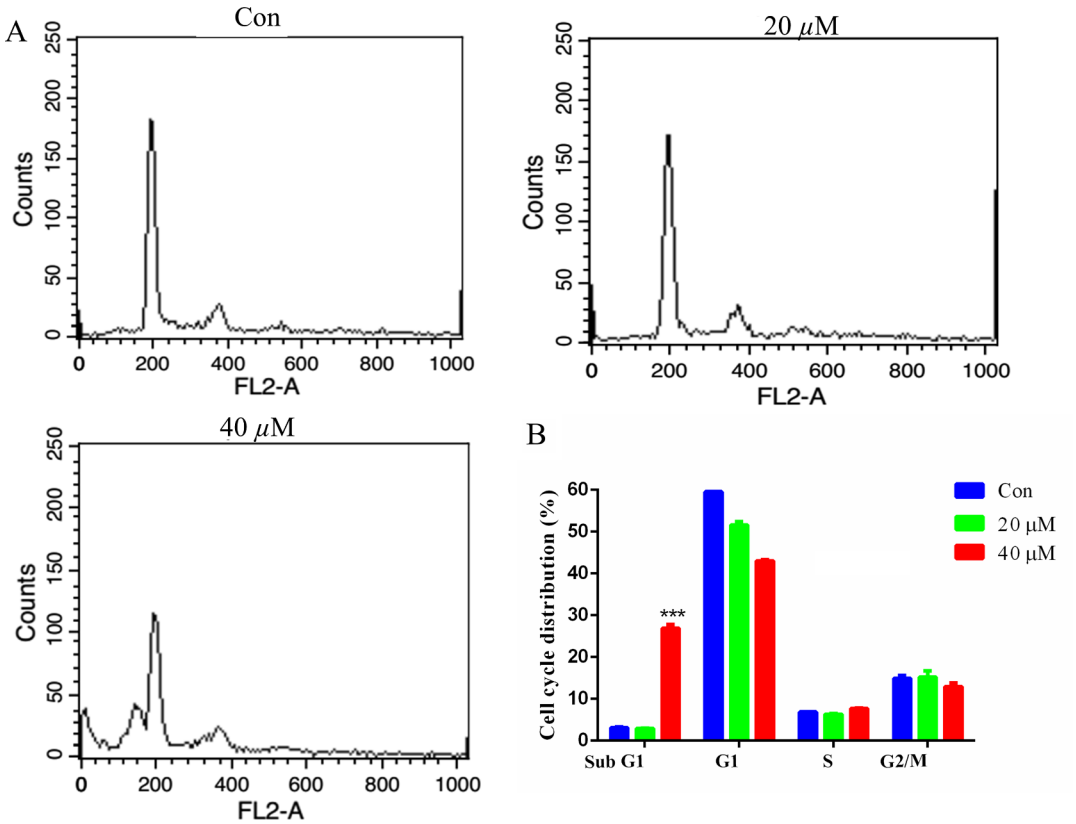

Fig. 8. Effects of compound **3** on cell cycle distribution. (A) Cell cycle histograms of HepG2 cells assessed by flow cytometry. (B) Quantification of HepG2 cells at each stage of the cell cycle after treatment with **3**. ***$p < 0.001$, as compared with the control.

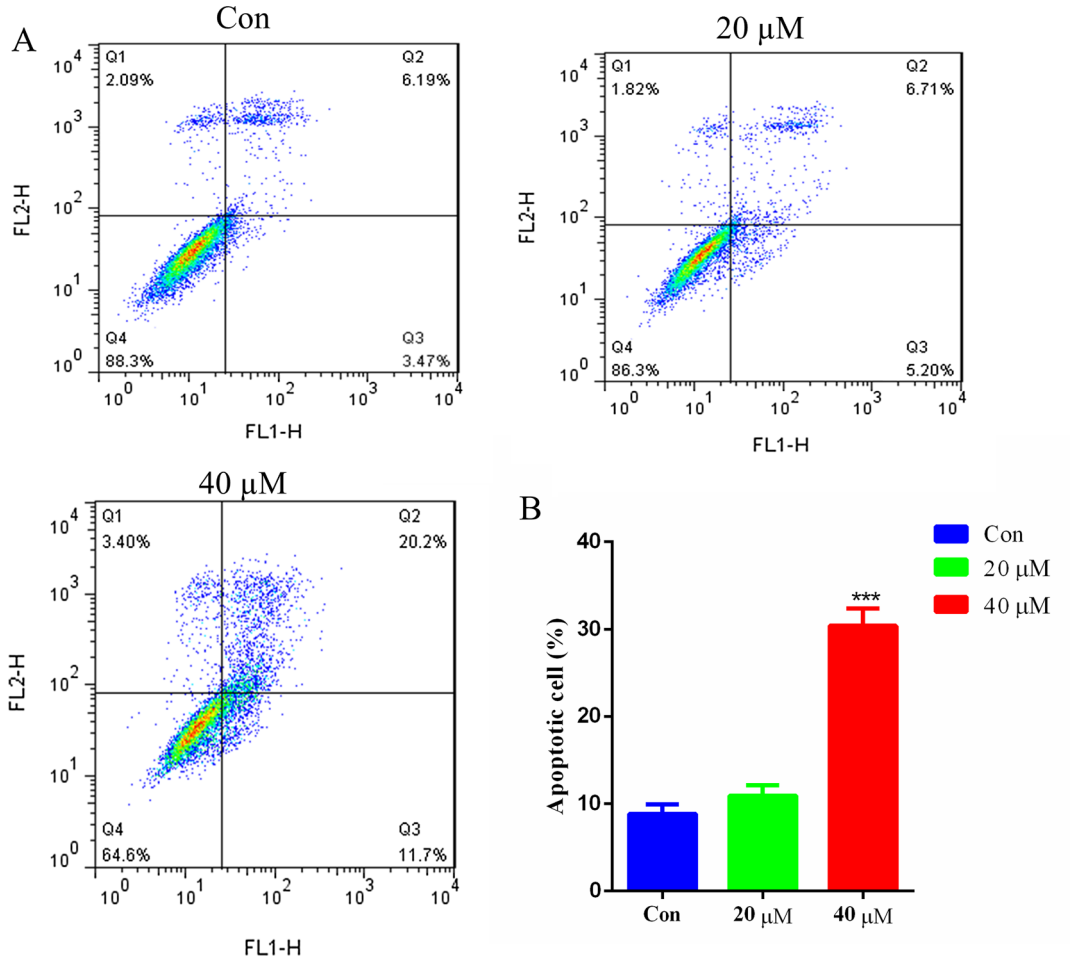

Fig. 9. Apoptosis induced by compound **3** in HepG2 cells. (A) Flow cytometry analysis of Annexin V-FITC/PI-stained HepG2 cells for 48 h. (B) Quantitative analysis of the ratio of apoptotic HepG2 cells. ***$p < 0.001$ compared with control.

Conflict of interest

All authors declare no conflict of interest.

Acknowledgement

This study was financially supported by the National Nature Science Foundation (81872767) of the People's Republic of China.

Appendix A. Supplementary material

Supplementary data to this article can be found online at https://doi.org/10.1016/j.bioorg.2018.11.049.

References

[1] S.K. Chen, B.Y. Chen, Chinese Flora, Science Press, Beijing, 1997.
[2] J. Xu, D. Xiao, W. Song, L. Chen, W. Liu, N. Xie, F. Feng, W. Qu, Quassinoids from the stems of *Picrasma quassioides* and their cytotoxic and NO production-inhibitory activities, Fitoterapia 110 (2016) 13–19.
[3] W. Jiao, G.D. Chen, H. Gao, J. Li, B. Gu, T. Xu, H. Yu, G. Shi, F. Yang, X. Yao, H. Lin, (±)-Quassidines I and J, two pairs of cytotoxic bis-β-carboline alkaloid enantiomers from *Picrasma quassioides*, J. Nat. Prod. 77 (12) (2014) 2707–2712.
[4] Z. Lai, W. Liu, S. Ip, H. Liao, Y. Yi, Z. Qin, X. Lai, Z. Su, Z. Lin, Seven alkaloids from *Picrasma quassioides* and their cytotoxic activities, Chem. Nat. Compd. 50 (5) (2014) 884–888.
[5] S. Yang, J. Yue, Five new quassinoids from the bark of *Picrasma quassioides*, Helv. Chim. Acta 87 (6) (2004) 1591–1600.
[6] Z.L. Hong, J. Xiong, S.B. Wu, J.J. Zhu, J.L. Hong, Y. Zhao, G. Xia, J.F. Hu, Tetracyclic triterpenoids and terpenylated coumarins from the bark of *Ailanthus altissima* ("Tree of Heaven"), Phytochemistry (Elsevier) 86 (2013) 159–167.
[7] J. Xu, D. Xiao, Q. Lin, J. He, W. Liu, N. Xie, F. Feng, W. Qu, Cytotoxic tirucallane and apotirucallane triterpenoids from the stems of *Picrasma quassioides*, J. Nat. Prod. 79 (8) (2016) 1899–1910.
[8] R.A. Hill, J.D. Connolly, Triterpenoids, Nat. Prod. Rep. 30 (7) (2013) 1028–1065.
[9] W.Y. Zhao, X.Y. Shang, L. Zhao, G.D. Yao, Z. Sun, X.X. Huang, S.J. Song, Bioactivity-guided isolation of β-carboline alkaloids with potential anti-hepatoma effect from *Picrasma quassioides* (D. Don) Benn, Fitoterapia 130 (2018) 66–72.
[10] B. Jagannadh, S.S. Reddy, R.P. Thangavelu, Conformational preferences of 1,4,7-trithiacyclononane: a molecular mechanics and density functional theory study, J. Mol. Model. 10 (1) (2004) 55–59.
[11] G.W.T.M.J. Frisch, H.B. Schlegel, G.E. Scuseria, M.A. Robb, J.R. Cheeseman, G. Scalmani, V. Barone, G.A. Petersson, H. Nakatsuji, X. Li, M. Caricato, A. Marenich, J. Bloino, B.G. Janesko, R. Gomperts, B. Mennucci, H.P. Hratchian, J.V. Ortiz, A.F. Izmaylov, J.L. Sonnenberg, D. Williams-Young, F. Ding, F. Lipparini, F. Egidi, J. Goings, B. Peng, A. Petrone, T. Henderson, D. Ranasinghe, V.G. Zakrzewski, J. Gao, N. Rega, G. Zheng, W. Liang, M. Hada, M. Ehara, K. Toyota, R. Fukuda, J. Hasegawa, M. Ishida, T. Nakajima, Y. Honda, O. Kitao, H. Nakai, T. Vreven, K. Throssell, J.A. Montgomery Jr., J.E. Peralta, F. Ogliaro, M. Bearpark, J.J. Heyd, E. Brothers, K.N. Kudin, V.N. Staroverov, T. Keith, R. Kobayashi, J. Normand, K. Raghavachari, A. Rendell, J.C. Burant, S.S. Iyengar, J. Tomasi, M. Cossi, J.M. Millam, M. Klene, C. Adamo, R. Cammi, J.W. Ochterski, R.L. Martin, K. Morokuma, O. Farkas, J.B. Foresman, D.J. Fox, Gaussian 09, Gaussian Inc, Wallingford CT, 2016.
[12] A. Merrien, J. Polonsky, The natural occurrence of melianodiol and its diacetate in *Samadera madagascariensis* (simaroubaceae): model experiments on melianodiol directed towards simarolide, J. Chem. Soc. D: Chem. Commun. 6 (1971) 261–263.
[13] J. Puripattanavong, S. Weber, V. Brecht, A.W. Frahm, Phytochemical investigation of *Aglaia andamanica*, Planta Med. 66 (08) (2000) 740–745.
[14] H.L. Huang, C.M. Wang, Z.H. Wang, M.J. Yao, G.T. Han, J.C. Yuan, K. Gao, C.S. Yuan, Tirucallane-type triterpenoids from *Dysoxylum lenticellatum*, J. Nat. Prod. 74 (10) (2011) 2235–2242.
[15] T. Nakanishi, A. INADA, D. LAvIE, A new tirucallane-type triterpenoid derivative, lipomelianol from fruits of *Melia toosendan* sieb. et zucc, Chem. Pharm. Bull. 34 (1) (1986) 100–104.
[16] S. Takahashi, H. Satoh, Y. Hongo, H. Koshino, Structural revision of terpenoids with a (3Z)-2-methyl-3-penten-2-ol moiety by the synthesis of (23E)- and (23Z)-cycloart-

23-ene-3 beta,25-diols, J. Org. Chem. 72 (12) (2007) 4578–4581.
[17] Y. Niimi, H. Hirota, T. Tsuyuki, T. Takahashi, New 7,24-tirucalladiene-type triterpenoids from *Picrasma quassioides* Bennett, Chem. Pharm. Bull. 37 (1) (1989) 57–60.
[18] W.R. Chan, D.R. Taylor, T. Yee, Triterpenoids from *Entandrophragma cylindricum*. I structures of sapelins A and B, J. Chem. Soc. C 2 (1970) 311–314.
[19] V. Kumar, N.M.M. Niyaz, D.B.M. Wickramaratne, S. Balasubramaniam, Tirucallane derivatives from *Paramignya monophylla* fruits, Phytochemistry 30 (4) (1991) 1231–1233.
[20] C. Kamperdick, T.P. Lien, G. Adam, T.V. Sung, Apotirucallane and Tirucallane triterpenoids from *Luvunga sarmentosa*, J. Nat. Prod. 66 (5) (2003) 675–678.
[21] I.J. Lee, G.H. Xu, J.H. Ju, J.A. Kim, S.W. Kwon, S.H. Lee, S.B. Han, Y. Kim, 21-Methylmelianodiols from *Poncirus trifoliata* as inhibitors of interleukin-5 bioactivity in Pro-B cells, Planta Med. 74 (4) (2008) 396–400.
[22] X.D. Luo, S.H. Wu, Y.B. Ma, D.G. Wu, Tirucallane triterpenoids from *Dysoxylum hainanense*, Phytochemistry 54 (8) (2000) 801–805.
[23] P. Judith, V. Zoia, R.M. Rabanal, J. Henry, 21,20-Anhydromelianone and melianone from *Simarouba amara* (Simaroubaceae); carbon-13 NMR spectral analysis of Δ7-tirucallol-type triterpenes, Isr. J. Chem. 16 (1) (1977) 16–19.
[24] Z.L. Hong, J. Xiong, S.B. Wu, J.J. Zhu, J.L. Hong, Y. Zhao, G. Xia, J.F. Hu, Tetracyclic triterpenoids and terpenylated coumarins from the bark of *Ailanthus altissima* ("Tree of Heaven"), Phytochemistry 86 (2013) 159–167.
[25] S.D. Jolad, J.J. Hoffmann, J.R. Cole, M.S. Tempesta, R.B. Bates, Constituents of *Trichilia hispida* (Meliaceae). 2. A new triterpenoid, hispidone, and bourjotinolone A, J. Organ. Chem. 45 (15) (1980) 3132–3135.
[26] H. Itokawa, E. Kishi, H. Morita, K. Takeya, Cytotoxic quassinoids and tirucallane-type triterpenes from the woods of *Eurycoma longifolia*, Chem. Pharm. Bull. 40 (4) (1992) 1053–1055.
[27] R. Su, M. Kim, H. Kawaguchi, T. Yamamoto, K. Goto, T. Taga, Y. Miwa, M. Kozuka, S. Takahashi, Triterpenoids from the fruits of *Phellodendron chinense* Schneid.: the stereostructure of niloticin, Chem. Pharm. Bull. 38 (6) (1990) 1616–1619.
[28] H. Liu, J. Heilmann, T. Rali, O. Sticher, New tirucallane-type triterpenes from *Dysoxylum variabile*, J. Nat. Prod. 64 (2) (2001) 159–163.
[29] L. Pan, Y.W. Chin, H.B. Chai, T.N. Ninh, D.D. Soejarto, A.D. Kinghorn, Bioactivity-guided isolation of cytotoxic constituents of *Brucea javanica* collected in Vietnam, Bioorg. Med. Chem. 17 (6) (2009) 2219–2224.
[30] J.S. Zhang, Y. Zhang, S. Li, A. Ahmed, G.H. Tang, S. Yin, Cytotoxic macrocyclic diterpenoids from *Jatropha multifida*, Bioorg. Chem. 80 (2018) 511–518.